

ARTICLE

Received 15 Apr 2010 | Accepted 19 Jan 2011 | Published 15 Feb 2011

DOI: 10.1038/ncomms1202

I_h -mediated depolarization enhances the temporal precision of neuronal integration

Ivan Pavlov¹, Annalisa Scimemi^{1,†}, Leonid Savtchenko¹, Dimitri M. Kullmann¹ & Matthew C. Walker¹

Feed-forward inhibition mediated by ionotropic GABA_A receptors contributes to the temporal precision of neuronal signal integration. These receptors exert their inhibitory effect by shunting excitatory currents and by hyperpolarizing neurons. The relative roles of these mechanisms in neuronal computations are, however, incompletely understood. In this study, we show that by depolarizing the resting membrane potential relative to the reversal potential for GABA_A receptors, the hyperpolarization-activated mixed cation current (I_h) maintains a voltage gradient for fast synaptic inhibition in hippocampal pyramidal cells. Pharmacological or genetic ablation of I_h broadens the depolarizing phase of afferent synaptic waveforms by hyperpolarizing the resting membrane potential. This increases the integration time window for action potential generation. These results indicate that the hyperpolarizing component of GABA_A receptor-mediated inhibition has an important role in maintaining the temporal fidelity of coincidence detection and suggest a previously unrecognized mechanism by which I_h modulates information processing in the hippocampus.

¹ Department of Clinical and Experimental Epilepsy, UCL Institute of Neurology, London WC1N 3GB, UK. [†] Present address: Synaptic Physiology Section, National Institute of Neurological Disorders and Stroke, National Institutes of Health, Bethesda, Maryland 20892-3701, USA. Correspondence and requests for materials should be addressed to M.C.W. (email: mwalker@ion.ucl.ac.uk).

Microelectrode and electroencephalography studies show that groups of neurons can fire synchronously with millisecond precision¹. To maintain temporal fidelity of information encoding, neurons act predominantly as coincidence detectors rather than neuronal integrators². The precision of coincidence detection in pyramidal cells depends critically on feed-forward inhibition^{3,4}. Such inhibition, mediated by GABA_A receptors, acts both by shunting excitatory currents (shunting inhibition) and by hyperpolarizing neurons (voltage inhibition)⁵. Shunting inhibition reduces the amplitude and duration of excitatory postsynaptic potentials (EPSPs) by increasing the membrane conductance. The hyperpolarizing action of inhibitory postsynaptic potentials (IPSPs), on the other hand, offsets the depolarization mediated by EPSPs and is long lasting, resulting in a biphasic EPSP–IPSP sequence in many neurons⁵.

It has been suggested that the temporal precision of neuronal integration also depends on I_h , but this effect has been attributed to HCN-mediated shunting of excitatory inputs⁶. I_h is a mixed cationic current with a reversal potential of ~ -30 mV present in neurons throughout the brain (for reviews see refs 7, 8). As I_h is present at resting membrane potential, it depolarizes neurons^{9–11}. I_h has a marked effect on dendritic processing by directly shunting excitatory inputs^{12,13} and through interactions with other membrane conductances^{14,15}. Consequently, blocking I_h facilitates the temporal summation of EPSPs and action potential firing during repetitive stimulation^{12,13,16}. As I_h can also affect IPSP kinetics^{17,18}, we asked what effect I_h blockade has on coincidence detection, when inhibition is left intact.

Here, we report that blocking I_h results in a significant broadening of the window for neuronal integration. This, however, is not due to the influence of I_h on PSP kinetics, but rather is secondary to the hyperpolarizing effect of I_h blockade. Indeed, I_h is required to maintain the hyperpolarizing action of synaptically released GABA, and so, blocking I_h broadens the excitatory phase of the EPSP–IPSP sequence evoked by afferent stimulation. These results show an essential role for I_h in determining the relative values of the resting membrane potential (V_R) and the reversal potential for GABA_A receptor-mediated currents ($E_{GABA(A)}$), and also show that hyperpolarizing inhibition is necessary for temporally precise neuronal integration of synaptic inputs.

Results

Blocking I_h increases the integration time window. We assessed coincidence detection by recording from CA1 pyramidal cells

using gramicidin perforated-patch in current-clamp mode¹⁹. We stimulated two separate populations of Schaffer collaterals (Fig. 1a) representing weak and strong synaptic inputs (see Methods). The stimulus intensities were adjusted so that simultaneous activation of the two pathways resulted approximately in a 50% chance of the neuron spiking. We then measured the spike probability while systematically varying the interstimulus interval. As previously reported, the spike probability decreased as the interval increased (Fig. 1b,c). We used 10 μ M ZD-7288 to block I_h . Again consistent with previous studies^{9,10}, this resulted in a hyperpolarization, an increase in input resistance and complete disappearance of the characteristic depolarizing sag of the membrane potential following a hyperpolarizing step current injection (Supplementary Fig. S1). We then readjusted the stimulation intensities to match the spiking probability for simultaneous stimulation observed under control conditions. Blocking I_h resulted in a significant broadening of the

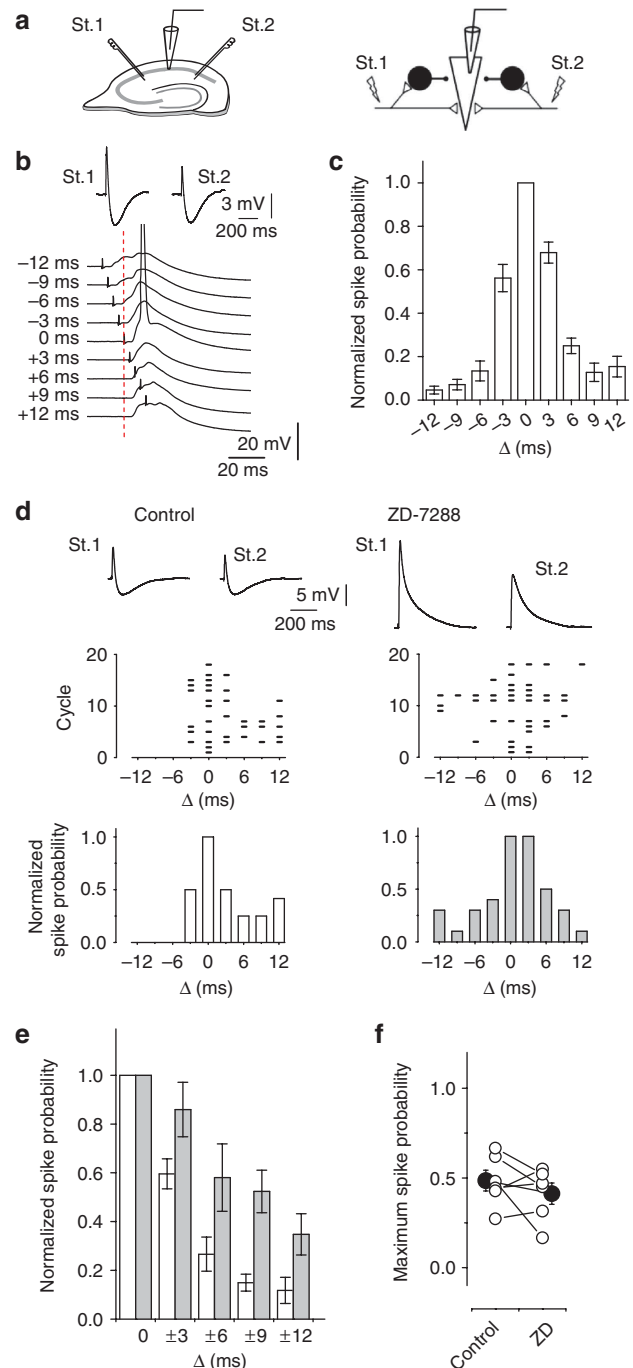


Figure 1 | Block of I_h widens the coincidence-detection time window.

(a) Two Schaffer collateral pathways (St.1 and St.2) were stimulated on either side of the recorded neuron ~ 300 μ m away from the soma to evoke EPSP–IPSP sequences. (b) Both pathways were then activated at different interstimulus intervals. Traces show sample responses. Stimulation intensities were adjusted so that the probability of evoking action potential was 50% when the two stimuli were delivered simultaneously. (c) Summary graph of probability of evoking an action potential against the interval between stimulations ($n = 19$). (d) Sample experiment demonstrating a change in the coincidence-detection time window following I_h blockade with ZD-7288. Top: Sample traces recorded in response to stimulation of two pathways in control and after application of ZD-7288; middle: raster plots of spike generation; bottom: frequency histograms showing spike probability at different intervals between stimuli. (e) Summary graph of relative probability of firing at different interstimulus intervals in control conditions (open columns) and in the presence of ZD-7288 (shaded columns; $n = 6$; $P = 0.011$ for difference). (f) The probability of evoking an action potential by simultaneous activation of both pathways under baseline conditions and after the readjustment of stimulus intensity following I_h block (open circles: individual recordings; closed circles: averaged data; $n = 6$). Error bars represent s.e.m.

time window for integration of the two input stimuli (Fig. 1d–f; $n=6$; repeated measures analysis of variance (ANOVA): $F(1,5)=15.5$, $P=0.011$). We further confirmed this effect using cell-attached recordings at near physiological temperature and with the same stimulation paradigm (Supplementary Fig. S2; $n=4$; repeated measures ANOVA: $F(1,3)=37.3$, $P=0.009$ for the effect of ZD-7288).

Blocking I_h prolongs excitation through hyperpolarization. Input summation in the above experiments depends on the time course of the EPSP–IPSP sequence^{4,19,20}. The long membrane time constant of hippocampal principal cells permits EPSP summation over a large time window, but disynaptic feed-forward inhibition limits the temporal summation of the excitatory inputs by curtailing the EPSPs^{4,19}. I_h could influence the EPSP–IPSP sequence profile by altering membrane conductance^{21,22}, interneuron recruitment²³ and/or V_R ^{9–11}. To address the relative roles of these effects of I_h , we evoked an EPSP–IPSP sequence in CA1 pyramidal cells by stimulating Schaffer collaterals, and then blocked I_h with and without correcting the membrane voltage (Fig. 2). Blocking I_h with ZD-7288 completely abolished the hyperpolarizing component of the EPSP–IPSP sequence and resulted in considerable broadening of the half-width of the depolarizing phase of the response to $251 \pm 27\%$ of control ($n=4$; $P=0.003$; Fig. 2a,b).

We first examined whether the effect of I_h block on the EPSP–IPSP sequence could be entirely accounted for by hyperpolarization of V_R . Following the application of ZD-7288, V_R was returned to the baseline level by injecting a constant current into the recorded neuron and the EPSP–IPSP sequence was again recorded (Fig. 2b). Almost full recovery of the hyperpolarizing phase of the response was observed ($80 \pm 8\%$ of the baseline amplitude before ZD-7288 application; $n=4$; $P=0.1$). In these experiments, there was only a relatively small increase in peak amplitude ($36 \pm 10\%$; $P=0.04$) and half-width ($39 \pm 9\%$; $P=0.02$) of the depolarization, consistent with some direct effect of I_h on the EPSPs; these effects were significantly smaller than those observed with the addition of ZD-7288 without current injection (that is, without correcting the neuronal hyperpolarization; $P=0.02$ and $P=0.004$ for amplitude and half-width of depolarizing phase of the EPSP–IPSP sequence, respectively (Fig. 2b)). The changes in the EPSP amplitude and half-width following ZD-7288 application and direct current injection (Fig. 2b) were similar to those observed when testing the effect of ZD-7288 on EPSPs when GABA_A receptors were also blocked with $100 \mu\text{M}$ picrotoxin (Fig. 2c, V_R was fixed at the control level with direct current injections). These results argue against a significant contribution of non-specific effects of ZD-7288 on presynaptic function²⁴. In addition, because of the limited space clamp in our experimental conditions (see Methods), recovery of the hyperpolarizing component of the postsynaptic response by current injection indicates that the majority of the inhibitory synapses recruited by Schaffer collateral stimulation impinge either close to the soma or on proximal dendrites of pyramidal cells. This is in line with previous findings that feed-forward inhibition in hippocampal CA1 pyramidal neurons underlying temporally precise synaptic integration is predominantly perisomatic⁴.

We further tested the effect of I_h block on GABA_A receptor-mediated transmission, as I_h has been reported to be present in some interneurons^{23,25,26}. We stimulated Schaffer collaterals and recorded in whole-cell voltage-clamp configuration with the membrane potential clamped to 0 mV (the reversal potential for glutamatergic currents) to isolate inhibitory postsynaptic current (IPSCs). Consistent with the results obtained in current clamp, ZD-7288 only reduced the IPSC amplitude by $17.5 \pm 3\%$ ($n=3$). The effect of I_h on the EPSP–IPSP sequence can therefore be largely attributed to the I_h -dependent depolarization of V_R and to the loss of the hyperpolarizing action of the IPSPs. Does shunting inhibition also modify the EPSP–IPSP sequence? To test this, we applied the GABA_A receptor antagonist

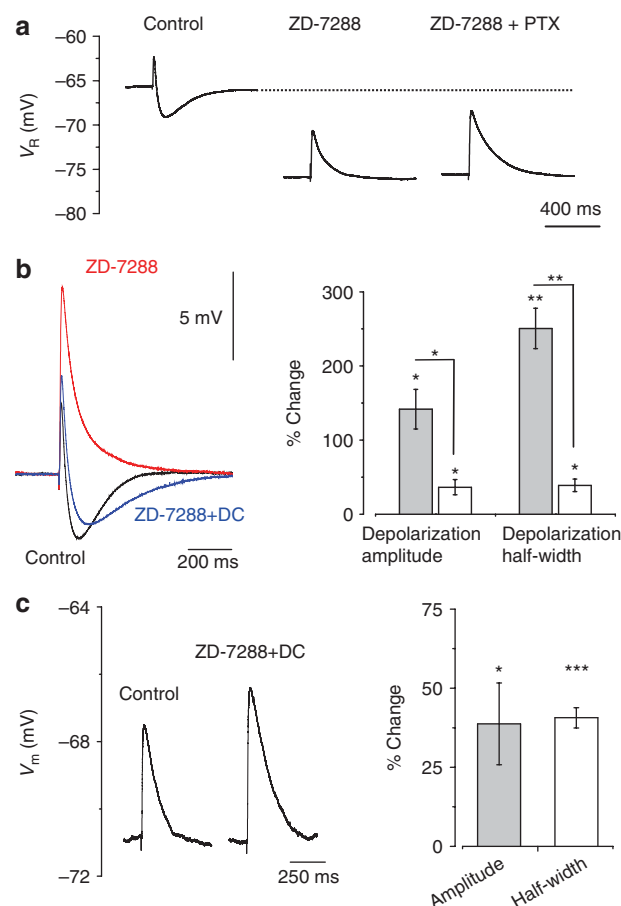


Figure 2 | I_h block abolishes the hyperpolarizing phase of the EPSP–IPSP sequence.

(a) EPSP–IPSP sequences were evoked in CA1 pyramidal cells by Schaffer collateral stimulation as in Figure 1. Consecutive traces from a representative experiment showing a shift in V_R following ZD-7288 application, associated abolition of the GABA_A receptor-mediated hyperpolarizing component of the EPSP–IPSP sequence (GABA_B receptors are blocked with $5 \mu\text{M}$ CGP52432) and the overall contribution of inhibition revealed by subsequent application of picrotoxin (PTX).

(b) Summary of ZD-7288 effect on EPSP–IPSP characteristics with (direct current (DC)) and without constant current injection to compensate for ZD-7288-induced shift in V_R ($n=4$ cells; shaded columns: ZD-7288, open columns: ZD-7288 + DC). Overlapped averaged traces are shown on the left (prepulse baseline is normalized). (c) Effect of application of ZD-7288 on the amplitude and duration of pharmacologically isolated EPSPs, while maintaining V_R with current injection ($n=7$; recordings were made in the presence of $5 \mu\text{M}$ CGP52432 and $100 \mu\text{M}$ picrotoxin); this effect is similar to the effect of ZD-7288 on the EPSP–IPSP sequence + DC (b). Bar charts represent percentage change of control values; error bars represent s.e.m.; * $P<0.05$, ** $P<0.01$, *** $P<0.001$.

picrotoxin with I_h blocked. This resulted in further prolongation of the EPSPs, indicating an additional role of shunting inhibition in regulating the shape of the EPSP–IPSP sequence (Fig. 2a).

One prediction from these results is that genetic ablation of I_h should similarly hyperpolarize neurons, change the driving force for chloride and prolong the depolarizing phase of the EPSP–IPSP sequence. We examined HCN1 knockout mice and compared them with wild-type littermate controls. Consistent with previous studies^{27,28}, HCN1 knockouts lacked the I_h -mediated membrane potential sag following hyperpolarizing step current injection (Fig. 3a). The resting membrane potential of pyramidal cells was more hyperpolarized in the knockout mice ($-72.6 \pm 2.5 \text{ mV}$) compared with

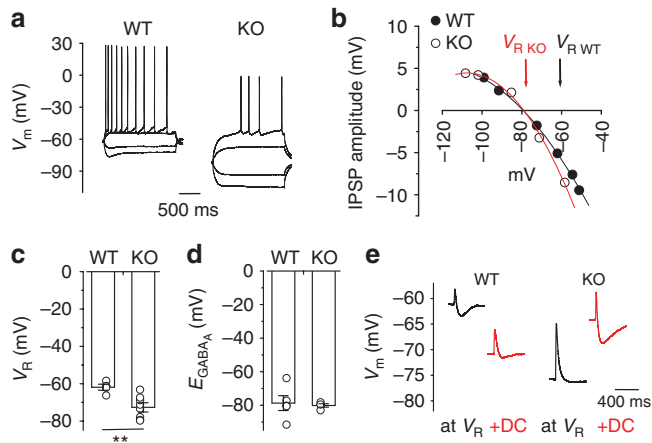


Figure 3 | HCN1 deletion results in the loss of the hyperpolarizing effects of GABA_A receptor-mediated inhibition. (a) Example traces showing voltage responses to current steps injections in wild-type (WT) mice and HCN1 knockout (KO) mice. (b) An example plot showing that, unlike WT mice, HCN1 KO mice lacked a hyperpolarizing GABA_A receptor-mediated driving force. Data points were fitted with a second-order polynomial function. (c) Comparison of V_R in HCN1 KO mice and WT mice (WT: $n=5$; KO: $n=8$). (d) Summary plot of $E_{GABA(A)}$ in both genotypes (WT: $n=5$; KO: $n=4$). (e) Sample traces showing that the KO mice displayed no hyperpolarizing phase at V_R , whereas WT animals had a biphasic EPSP-IPSP sequence. The hyperpolarizing IPSPs became apparent in the KO mice when cells were depolarized by DC injection. Conversely, the IPSP was less evident when pyramidal cells from WT mice were hyperpolarized. Error bars represent s.e.m.; ** $P<0.01$.

wild-type littermate control animals (-61.9 ± 1.6 mV; $P=0.0037$; Fig. 3a–c); however, $E_{GABA(A)}$ was similar in both genotypes (Fig. 3b,d). As predicted, the hyperpolarizing phase of the EPSP-IPSP sequence was either absent or reduced in the knockout animals, and the width of the EPSPs was broadened to $193.4 \pm 18.4\%$ of the wild-type value ($P=0.009$; Fig. 3e).

I_h maintains V_R more depolarized than $E_{GABA(A)}$. The results thus far indicate that I_h -dependent neuronal depolarization is necessary to maintain a hyperpolarizing effect of GABA_A receptor currents. We directly tested this hypothesis using gramicidin perforated-patch current-clamp recordings, which minimize perturbation of the internal Cl^- concentration. $E_{GABA(A)}$ was determined from the reversal potential of evoked IPSPs, and was uniformly negative to V_R (mean $E_{GABA(A)} - V_R$: -5.2 ± 1.0 mV; $n=12$; $P=0.0003$; Fig. 4a). In all cells, application of ZD-7288 resulted in a significant negative shift in V_R (-8.6 ± 0.9 mV; $P=7.4 \times 10^{-7}$; $n=12$; Fig. 4b,c). In contrast, inhibition of I_h led to only a small depolarizing shift in $E_{GABA(A)}$ (2.1 ± 0.8 mV; $P=0.03$; Fig. 4d). The net effect of blocking I_h was to make V_R more negative than $E_{GABA(A)}$ in 10 out of 12 cells (mean $E_{GABA(A)} - V_R$: 5.5 ± 1.3 mV; $n=12$; $P=0.0013$; Fig. 4e). This demonstrates a major role of I_h in maintaining a hyperpolarizing driving force for fast GABAergic transmission.

Correcting V_R after I_h block restores coincidence detection. Although the broadening of input integration is consistent with the hypothesis that GABA_A receptor-mediated hyperpolarization is required to maintain the narrow time window for coincidence detection, an alternative potential explanation is that I_h has a profound effect upon dendritic excitability and temporal summation of excitatory inputs^{12,13}. To distinguish between these hypotheses, we repeated the coincidence-detection experiments, but depolarized the neuron following addition of ZD-7288 to return the resting

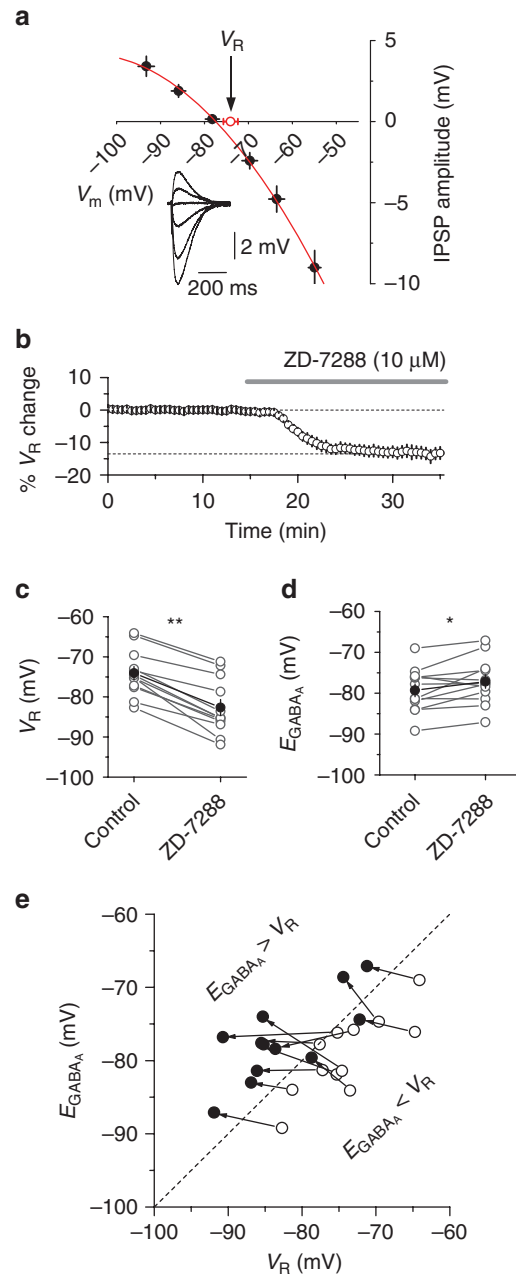


Figure 4 | Blocking I_h changes the V_R - $E_{GABA(A)}$ relationship in CA1 pyramidal cells. (a) In control conditions, all cells had negative $E_{GABA(A)}$ compared with V_R ($n=12$). Sample IPSPs at different membrane potentials from a typical experiment are shown in the inset. Data points were fitted with a second-order polynomial function. (b) Time course of the changes in V_R following the application of ZD-7288 ($n=12$). (c) Effect of ZD-7288 on V_R (filled circles are mean values, open circles are data from individual experiments; $n=12$). (d) Effect of I_h block on $E_{GABA(A)}$ (filled circles are mean values, open circles are data from individual experiments; $n=12$). (e) Summary graph showing the effect of ZD-7288 on $E_{GABA(A)}$ and V_R . $E_{GABA(A)}$ became more depolarized than V_R in 10 out of 12 cells (open circles: control, filled circles: in ZD-7288). Error bars represent s.e.m.; * $P<0.05$, ** $P<0.01$.

membrane potential to the baseline level. Using this protocol, we observed no change in the time window for integration (Fig. 5; $n=5$; repeated measures ANOVA: $F(1,4)=0.374$, $P=0.57$). This implies that it is primarily the depolarizing effect of I_h and loss of the hyperpolarizing effect of GABA_A receptor currents that maintains the narrow coincidence detection for input integration. A further

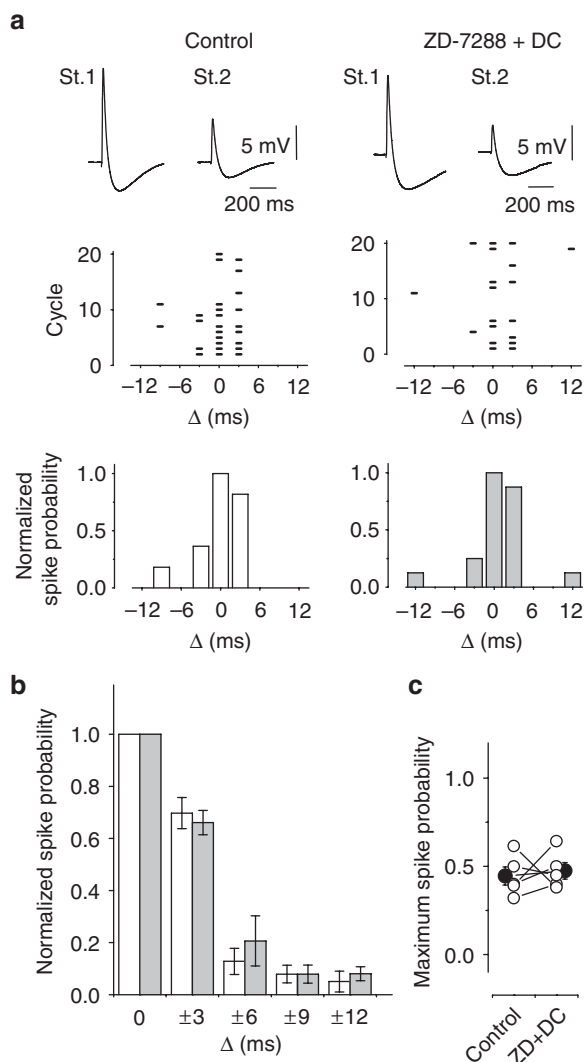


Figure 5 | Repolarization restores temporal precision when I_h is blocked.

(a) Spike probability at different intervals between stimuli in control conditions and in the presence of ZD-7288 when neurons were repolarized to their initial V_R by DC injection, therefore restoring the biphasic shape of the EPSP-IPSP sequence. Top: sample traces; middle: raster plots of spikes initiated by stimulation of the two pathways at different delay intervals; bottom: spike probability distribution graphs. (b) Averaged data from five experiments (open columns: control, shaded columns: ZD-7288 + DC; $P=0.57$). (c) Probability of action potential generation for synchronous stimulation of both pathways before and after application of ZD-7288 ($n=5$). Error bars represent s.e.m.

prediction from this is that simple hyperpolarization with I_h intact would widen the coincidence-detection time window, which is indeed the case ($n=5$, repeated measures ANOVA: $F(1,4)=8.2$, $P=0.046$; Supplementary Fig. S3).

Hyperpolarizing inhibition underlies temporal precision. A possible confounder in the above experiments is that in order to maintain a 50% spiking probability, we had to adjust the stimulation intensity to compensate for the membrane hyperpolarization, potentially affecting interneuron recruitment. This would tend to increase the interneuron recruitment and therefore would be expected to narrow the integration time window (in contrast to the broadening that we observed). Nevertheless, to control for this and to address the question of whether loss of the hyperpolarization effect of GABA_A

receptor currents is sufficient to explain our results, we constructed a simple integrate-and-fire model of a neuron that receives two inputs. Each input consisted of an excitatory followed by an inhibitory conductance, and the parameters were adjusted to simulate the kinetics of the experimentally obtained EPSP-IPSP sequence waveform (see Methods; Fig. 6a). In agreement with the experimental findings, systematic variation of the delay between the two inputs revealed a narrow integration time window for spike generation (Fig. 6b).

Hyperpolarization of V_R broadens the integration time window. Removing I_h from the modelled cell, hyperpolarized the membrane from -70 to -80 mV and led to an increase in the width of the integration time window (Fig. 6c; the area under the spike probability curve was increased by $26.3 \pm 2.3\%$; $P < 0.01$). This effect was robust and relatively insensitive to varying EPSP and IPSP kinetic parameters, delay times between excitatory and inhibitory synapse activation, as well as synapse locations on the dendrites (Supplementary Fig. S4). We also systematically changed the maximal probability of action potential generation to test whether this could affect our experimental results. The effect of membrane potential hyperpolarization was constant across a wide range of tested probability values (Supplementary Fig. S5).

To determine whether the effect on the integration window in the simulations was due to the conductance or voltage effect of I_h removal, we repolarized the neuronal soma back to -70 mV by introducing a depolarizing current. In agreement with experimental observations, this restored the width of the time window for integration, indicating a crucial role for the depolarizing action of I_h (Fig. 6d).

We next asked whether the effect that we observed was due to the voltage change itself rather than the change in the polarity of GABA_A receptor-mediated transmission. We therefore assessed the effects of membrane potential on the integration time window in the absence of GABAergic transmission. As expected⁴, removing feed-forward inhibition broadened the integration time window by $106.8 \pm 6.7\%$. However, the width of the window was minimally affected by changes in V_R in the range observed in our experiments and simulations (Fig. 7a; an increase of $3.1 \pm 0.4\%$ with 10 mV hyperpolarization).

In the above simulations, the magnitude of the inhibitory synaptic conductance was fixed to match the simulated EPSP-IPSP waveform with that observed experimentally. We therefore tested the effect of different inhibitory synaptic conductances. In all instances, hyperpolarizing V_R , so that the IPSPs became depolarizing, widened the integration time window. This effect initially increased with increases in the IPSP amplitude (Fig. 7b) up to a maximum and then decreased probably because of the increasing shunting versus voltage effect of inhibitory synapses.

Finally, we considered the possible confounding effect of variability in the size of the inhibitory conductance. At high stimulation intensity, the inhibitory conductance is relatively invariant²⁹. However, at lower stimulation intensities, inhibitory conductances vary with stimulation intensity (and magnitude of excitatory conductance). We therefore covaried the conductances of excitatory and inhibitory synapses (see Methods) to model this situation. Under these conditions, the window of integration was still increased following hyperpolarization of the neuron by $38.1 \pm 11.4\%$ compared with $20.2 \pm 2.6\%$, with constant inhibitory synaptic conductances (Fig. 7c; $P < 0.05$).

Discussion

We have shown that I_h is necessary to maintain a hyperpolarizing driving force for GABA_A receptor-mediated transmission by depolarizing the resting membrane potential of pyramidal cells. Hyperpolarizing the resting membrane potential through pharmacological inhibition of I_h or deletion of HCN1 results in depolarizing GABA_A receptor-mediated potentials and broadening of the excitatory phase

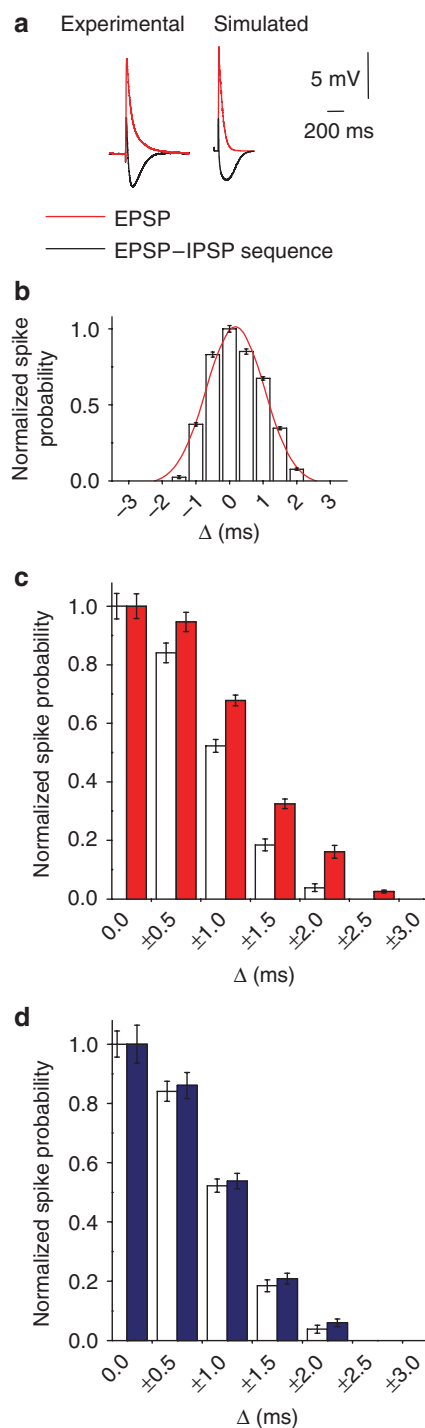


Figure 6 | I_h -mediated hyperpolarization broadens the integration time window in an integrate-and-fire neuronal model.

(a) Successive activation of excitatory and inhibitory conductances in a simple integrate-and-fire neuron was used to produce an EPSP-IPSP sequence similar to that observed experimentally. (b) Simulation of two pathways activated with different delays (see Methods) resulted in a narrow integration time window. Synaptic strength was adjusted so that the peak probability of action potential generation remained at 50%. (c) Removal of I_h from the dendrites hyperpolarized the modelled neuron by 10 mV. The graph shows spike probability at different intervals between stimuli with (open bars) and without I_h (red bars) in the modelled neuron. (d) The effect of I_h removal was abolished when the neuronal soma was repolarized by DC injection (open bars: control with I_h , blue bars: no I_h repolarized). Data are presented as means of 30 rounds of simulations, error bars represent s.e.m.

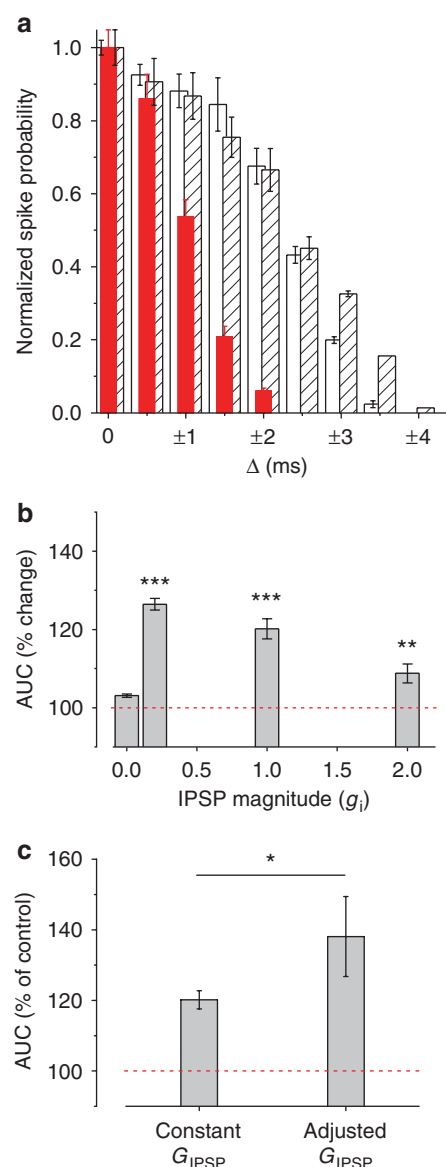


Figure 7 | The effects of changing the magnitude of inhibitory conductances on the width of the integration time window.

(a) In the absence of feed-forward inhibition (no IPSPs), the integration time window became broader. Under such conditions, membrane hyperpolarization did not change the width of coincidence detection, indicating that changes in the polarizing effect of GABA_A receptor-mediated currents, rather than the V_m value itself, determine neuronal integration (open bars: $V_m = -70$ mV no IPSP; hatched bars: $V_m = -80$ mV no IPSP; red bars: $V_m = -70$ mV with IPSP). (b) The effect of varying the strength of inhibitory connections on the width of the integration time window assessed as the change in the area under the spike probability curve (AUC). (c) The effect of hyperpolarization on the coincidence-detection time window when inhibitory synaptic conductances were scaled with excitatory conductances, mimicking the situation when inhibitory inputs onto a neuron are not saturated. Data are presented as means of 30 rounds of simulations, error bars represent s.e.m.; * $P < 0.05$, ** $P < 0.01$, *** $P < 0.001$.

of the EPSP-IPSP sequence, leading to a prolonged time window for synaptic integration. These results also demonstrate an important and unexpected role of voltage inhibition.

I_h channels are densely expressed in the dendritic arbour of CA1 pyramidal cells²¹. A significant proportion of these channels is active

at rest, reducing the membrane resistance and neuronal time constant. These effects of I_h have been shown to determine the time course of EPSPs onto CA1 pyramidal cells¹². The previous studies have concentrated on the impact of I_h on the integration properties of excitatory inputs, with GABA_A receptor-mediated inhibition blocked. However, GABAergic inhibition has a profound effect on the width of the integration time window of excitatory inputs⁴. The relative roles of shunting and hyperpolarizing inhibition in maintaining precise coincidence detection have not been addressed. Although one study has considered the effect of I_h on the integration time window without GABA_A receptor blockade⁶, that work was performed in whole-cell mode, with the membrane potential of the neurons fixed and the reversal potential of GABA_A responses set to be depolarizing.

In hippocampal neurons, $E_{\text{GABA(A)}}$ is negative to V_R by the end of the second postnatal week³⁰, so that GABA_A receptor-mediated potentials predominantly hyperpolarize the postsynaptic membrane in adult tissue, for example, see ref. (31). In adult neurons, $E_{\text{GABA(A)}}$ is mainly determined by the Cl⁻ cotransporter KCC2, which uses the transmembrane K⁺ gradient to maintain a low intracellular Cl⁻ concentration, thereby clamping the reversal potential for Cl⁻ (E_{Cl}) closer to that of K⁺ (E_K)³⁰. $E_{\text{GABA(A)}}$ is, however, more depolarized than E_{Cl} due to the permeability of the GABA_A receptors to HCO₃⁻ ions³². Therefore, to maintain hyperpolarizing IPSPs, V_R also has to be depolarized relative to $E_{\text{GABA(A)}}$. A number of conductances may contribute to this depolarization (such as persistent sodium currents and leak conductances); in CA1 pyramidal cells, I_h provides a significant depolarizing drive at resting membrane potential¹¹. In our study, this effect of I_h was more evident with pharmacological block than with genetic ablation, perhaps because of compensatory changes in other conductances in the HCN1 knockout mice.

We have shown that I_h sets the polarity of GABAergic events by making V_R more depolarized than $E_{\text{GABA(A)}}$, and most of the effects of I_h on the EPSP–IPSP sequence can be rescued by repolarizing V_R to its baseline value, arguing for a major role of GABAergic voltage inhibition in regulating the integration properties of synaptic inputs of CA1 pyramidal cells. As observed in our study and in other studies, for example, see ref. (33), GABA_A receptor activation can still shunt EPSPs even when $E_{\text{GABA(A)}}$ is more depolarized than V_R . However, the relative importance of shunting and hyperpolarizing effects of inhibition for neuronal computations and precise timing of action potential generation has received much less attention. Some experimental and theoretical studies have suggested that the hyperpolarizing effects of GABAergic neurotransmission are critical for network synchronization, for example, see ref. (34), whereas others emphasize the role of shunting inhibition in oscillatory behaviour of interconnected neurons³⁵. The ability of I_h to switch the inhibitory mode of GABAergic signals from hyperpolarizing to shunting or depolarizing adds further complexity in defining the computational properties of hippocampal neurons³⁶.

Further, it might be expected that the large, early shunting effect of GABAergic inhibition has the predominant part in curtailing the EPSPs. Our results, however, underscore the contribution of GABA_A receptor-mediated hyperpolarization in determining the temporal precision of coincidence detection by hippocampal pyramidal neurons. How does changing the GABA_A receptor-mediated response from hyperpolarizing translate to an increased integration time? Although shunting is maintained regardless of the polarization of GABA_A receptor-mediated responses (see Fig. 2a) attenuating the EPSPs generated in response to the second stimulation, this attenuation would be much stronger when the IPSP produces hyperpolarization. More importantly, because the voltage effect of an IPSP outlasts its shunting effect³³, it would have an impact on the excitatory potentials over an extended period. In the situation when the hyperpolarizing phase of the GABAergic response is abolished (and even more so if the polarity of the GABA_A response is changed), this

would facilitate EPSP summation. Therefore, the hyperpolarization that results from inhibition of I_h results in a considerable increase in the half-width of the time window for coincidence detection. Inhibition of other membrane conductances through hyperpolarization cannot account for this, as voltage changes of similar magnitudes, when I_h is blocked, result in minimal change in the membrane resistance or time constant¹¹. The critical role of hyperpolarization for coincidence detection has extensive implications, as anything that alters the polarity of GABA_A receptor-mediated transmission will affect the time window for input integration. This would include either a shift in $E_{\text{GABA(A)}}$ (for example, due to loss or inhibition of KCC2) or changes in resting membrane potential mediated through, for example, changes in membrane potassium conductances.

We have therefore shown the critical role of GABA_A receptor-mediated hyperpolarization in information processing and an unexpected mechanism by which I_h can modulate coincidence detection. As I_h is regulated by developmental³⁷, physiological³⁸ and pathological processes^{16,39–42}, such processes may consequently affect the properties of GABA_A receptor-mediated signalling and the temporal fidelity of coincidence detection. This may contribute to cognitive and psychiatric consequences of epilepsy by increasing the probability of aberrant associations. Moreover, the magnitude of somatic I_h is dependent upon excitatory synaptic activity, and this has been proposed to be a homeostatic mechanism regulating neuronal excitability³⁸. We further hypothesize that such a mechanism may have an additional homeostatic role by narrowing the time window for coincidence detection with increases in neuronal activity and conversely broadening the time window for integration when synaptic activity decreases. The role of I_h in restricting temporal input integration may also contribute to explaining the enhanced learning behaviour observed in HCN1 knockout mice²⁷, which may occur at the expense of loss of temporal discrimination of inputs.

Methods

Electrophysiology. We used transverse hippocampal slices (350 μm) from 3–6-week-old male Sprague–Dawley rats, or HCN1 knockout mice and their wild-type littermate controls. The HCN1 knockout animals were re-derived from that described previously, and maintained on a 129SVEV background^{27,28}.

Animals were killed according to schedule 1 of the UK Animals (Scientific Procedures) Act 1986. The brains were rapidly removed, dissected and cut with Leica VT1000S vibratome in ice-cold solution containing (in mM) sucrose (70), NaCl (80), KCl (2.5), MgCl₂ (7), CaCl₂ (0.5), NaHCO₃ (25), NaH₂PO₄ (1.25) and glucose (22), and were equilibrated with 95% O₂/5% CO₂ (pH 7.4). The slices were allowed to recover in an interface chamber (>1 h) at room temperature before being transferred to the recording chamber. Storage and perfusion solutions contained (in mM) NaCl (119), KCl (2.5), MgSO₄ (1.3), CaCl₂ (2.5), NaHCO₃ (26.2), NaH₂PO₄ (1) and glucose (22), and were gassed with 95% O₂/5% CO₂. All recordings, except for those in Figures 1, 5 and Supplementary Figure S3, were carried out at 32 °C. Current-clamp whole-cell recordings (Supplementary Fig. S1) were performed using pipettes (3–5 MΩ) filled with an intracellular solution containing (in mM) K-gluconate (145), NaCl (8), KOH–HEPES (10), EGTA (0.2), Mg-ATP (2) and Na₃-GTP (0.3); pH 7.2; 290 mOsm. Gramicidin (50 μg ml⁻¹) was added for perforated-patch recordings⁴³, and patch pipettes (8–12 MΩ) were front-filled with gramicidin-free solution; either QX-314 Br (5 mM) was added or [Cl⁻] was increased to 26 mM ($E_{\text{Cl}} = -41$ mV) to monitor patch integrity. Series resistance was monitored throughout. Data acquisition began when the series resistance was <150 MΩ (15–20 min after obtaining cell-attached configuration). To isolate GABA_A receptor-mediated IPSPs, NMDA, AMPA and GABA_A receptors were blocked with AP5 (50 μM), NBQX (20 μM) and CGP52432 (5 μM), respectively. Constant current stimuli were delivered to Schaffer collaterals through bipolar stainless steel electrodes placed in stratum radiatum. Monosynaptic IPSPs were evoked by positioning the stimulating electrode close to the recording site. EPSP–IPSP sequences were evoked by positioning the electrodes in stratum radiatum at least 300 μm away from the recording site; CGP52432 (5 μM) was added to the perfusate. Although application of CGP52432 reduced the duration of the hyperpolarizing phase by 16 ± 3% (Supplementary Fig. S6a–c), it did not affect the depolarizing component.

Two Schaffer collateral pathways were stimulated for the coincidence-detection protocol (Figs 1 and 5, Supplementary Fig. S3). Experiments were performed in the presence of 50 μM AP5 (to avoid spike timing-dependent plasticity) and 5 μM CGP52432. AP5 had a minimal impact on the excitatory phase of the EPSP–IPSP sequence, decreasing the half-width by 14 ± 4% (more than an order of magnitude smaller than the impact of changing the polarity of GABA_A responses; Supplementary

Fig. S6d–f). To ensure recording stability, these experiments were performed at room temperature (23–25°C); this increased the time course of the synaptic responses (Supplementary Fig. S7), but the shape of the EPSP–IPSP waveform was maintained. Although modelling indicated that this does not qualitatively change the experimental findings (Supplementary Fig. S4a), we confirmed this with cell-attached recordings at 32°C (Supplementary Fig. S2). These experiments were performed using patch pipettes (8–12 MΩ) filled with ACSF in voltage-clamp with the voltage set so that no current was injected under baseline conditions. As afferent input strength to the hippocampus can vary considerably, we stimulated a weak and a strong input; the amplitude of the response in one pathway was adjusted to be approximately twice that in the other pathway. In the cell-attached experiments, the ‘weak’ pathway was stimulated at approximately half-threshold intensity, whereas the ‘strong’ pathway stimulation was set close to the firing threshold. Stimulation intensities were adjusted to obtain ~50% spike probability when the two pathways were activated simultaneously. The two pathways were stimulated with an interstimulus delay varying from –12 to +12 ms in 3 ms steps (thus the order of inputs was reversed over the range investigated). To avoid any confounding effects of asymmetric distribution of spike probabilities, the data are presented as the averaged values from corresponding points on either side of the maximum.

In some experiments, constant current injection was used to repolarize the somatic membrane potential. Under our experimental conditions, there is a space clamp error in distal dendrites. However, as we observed experimentally that somatic current injection restored the hyperpolarization phase of the EPSP–IPSP waveform, we conclude that feed-forward inhibition in our study was predominantly perisomatic (Supplementary Fig. S8).

For experiments on the effect of I_h block on the magnitude of IPSCs, the intracellular solution contained (in mM) Cs-methanesulfonate (120), NaCl (8), HEPES (10), EGTA (0.2), $MgCl_2$ (0.2), Mg -ATP (2), Na -GTP (0.3) and QX-314 Br (5 mM); 290 mOsm. Schaffer collaterals were stimulated in the presence of AP5 and CGP52432. Neurons were voltage-clamped at 0 mV (close to the reversal potential for AMPA receptor-mediated response), and outward $GABA_A$ receptor-mediated currents were compared in the absence and presence of ZD-7288.

All recordings were obtained using a MultiClamp 700B amplifier (Molecular Devices), filtered at 2 kHz and digitized at 5 kHz. LabView (National Instruments) software was used for data acquisition and off-line analysis. Chemicals were purchased from Tocris Cookson or Sigma-Aldrich.

Modelling. All simulations were conducted with NEURON 7.0 (ref. 44) on a multimode cluster⁴⁵. The Hodgkin–Huxley neuron model consisted of a cylindrical soma (diameter = length = 20 μm) and two identical dendrites (3 μm diameter and 200 μm long). The axial resistance (R_a) was 35.4 Ohm cm^{–1}; membrane capacitance (C_m) was 1 μF cm^{–2}. The somatic membrane had Na^+ and K^+ conductances with the following peak values: $g_{Na} = 0.12$ S cm^{–2}, $g_K = 0.036$ S cm^{–2} ($E_K = -77$ mV and $E_{Na} = +50$ mV). The dendritic membrane had a passive leak current ($g_{pas} = 1$ mS cm^{–2} and $E_{pas} = -80$ mV) and I_h ($g_h = 1$ mS cm^{–2}, kinetics as in ref. 21). V_R was –70 mV. Removal of I_h hyperpolarized the neuron by 10 mV. In such conditions, 0.4 nA injected into the soma was necessary to repolarize the membrane potential to –70 mV. All simulations were performed with either $V_R = -70$ mV (baseline conditions) or –80 mV (hyperpolarized conditions).

Deterministic action potential generation was prevented by introducing Poisson-distributed conductances of uniformly distributed variable magnitude (0.9–1.1 nS; $\tau_{rise} = 0.1$ ms; $\tau_{decay} = 1$ ms; reversal potential = V_R to avoid significant membrane potential fluctuations) into the cell at a mean frequency of 1,000 Hz.

Each dendrite had a glutamatergic and GABAergic synapses, located at 180 and 40 μm from the soma, respectively. The dual-exponential formalism in the Exp2Syn function of neuron simulator was used to determine the time course of synaptic conductances:

$$g_s(t) = G_m(\exp(-t/\tau_1) - \exp(-t/\tau_2)), \quad (1)$$

where $g_s(t)$ is the synaptic conductance at time t after activation; τ_1 is the rise time constant (7 ms for glutamatergic synapses and 15 ms for GABAergic synapses); τ_2 is the decay time constant (35 ms for glutamatergic synapses and 50 ms for GABAergic synapses) and G_m is the value of the maximum synaptic conductance. To simulate the EPSP–IPSP sequence, there was a 7 ms delay from EPSPs to IPSPs. The reversal potentials were set at –75 and 0 mV for GABAergic and glutamatergic synapses, respectively.

The left excitatory and inhibitory synaptic conductances (G_{ESL} and G_{ISL}) were twice the right synaptic conductances (G_{ESR} and G_{ISR}). The onset time of the left EPSP–IPSP sequence was fixed whereas that of the right varied from –10 to +10 ms. To calculate the time distribution of the spike probability, interstimulus intervals were divided into 0.5 ms bins. The probability of action potential generation was determined using 30 rounds of ten synaptic stimulations with 500 ms interval between trials, initiated with a different seed. The interval between stimuli was sufficient to allow the model neuron to reach initial steady-state conditions. The mean number of action potentials per bin (M) and s.e. (ϵ) were calculated.

Area under the spike probability curve was used to quantify changes in the coincidence-detection time window. The s.e. of the surface under the distribution was defined as:

$$\epsilon = \frac{\text{bin} \cdot \sqrt{\sum_{i=1}^N \epsilon_i^2}}{p_{\max}}, \quad (2)$$

where N is the number of bins, bin is the bin size and p_{\max} is the maximum probability of the distribution.

The s.e. of the ratio of surfaces S1/S2 was defined as:

$$\epsilon_{ss} = \frac{S_1}{S_2} \sqrt{\left(\frac{\epsilon_1}{S_1}\right)^2 + \left(\frac{\epsilon_2}{S_2}\right)^2}. \quad (3)$$

The maximal probability of action potential generation (0.5) was set by scaling synaptic conductances with the parameter Stim: Stim $\times G_{ESL}$ and Stim $\times G_{ESR}$. The strengths of inhibitory synapses were set to $G_{ISL} = 450$ nS and $G_{ISR} = 225$ nS for left and right synapse, respectively, for the majority of simulations. For Figure 7b, the strength of inhibitory connections varied as indicated. For simulations presented in Figure 7c in addition to excitatory conductances, we also scaled inhibitory conductances: Stim $\times G_{ISL}$ and Stim $\times G_{ISR}$.

Simulations with maximal probabilities from 0.2 to 0.85 were performed (Supplementary Fig. S5). In these experiments, the actual maximal spike probability was determined *post hoc*.

Statistics. Two-tailed Student's t -test (paired or independent) and repeated measures ANOVA were used for statistical analysis. $P < 0.05$ for significant differences. Data are presented as mean \pm s.e.m.

References

- König, P., Engel, A. K. & Singer, W. Integrator or coincidence detector? The role of the cortical neuron revisited. *Trends Neurosci.* **19**, 130–137 (1996).
- Abeles, M. Role of the cortical neuron: integrator or coincidence detector? *Israel J. Med. Sci.* **18**, 83–92 (1982).
- Buzsáki, G. Feed-forward inhibition in the hippocampal formation. *Prog. Neurobiol.* **22**, 131–153 (1984).
- Pouille, F. & Scanziani, M. Enforcement of temporal fidelity in pyramidal cells by somatic feed-forward inhibition. *Science* **293**, 1159–1163 (2001).
- Eccles, J. The Ferrier lecture: the nature of central inhibition. *Proc. R. Soc. Lond. B* **153**, 445–476 (1961).
- Berger, T. & Luscher, H. R. Timing and precision of spike initiation in layer V pyramidal cells of the rat somatosensory cortex. *Cereb. Cortex* **13**, 274–281 (2003).
- Pape, H. C. Queer current and pacemaker: the hyperpolarization-activated cation current in neurons. *Annu. Rev. Physiol.* **58**, 299–327 (1996).
- Robinson, R. B. & Siegelbaum, S. A. Hyperpolarization-activated cation currents: from molecules to physiological function. *Annu. Rev. Physiol.* **65**, 453–480 (2003).
- Gasparini, S. & DiFrancesco, D. Action of the hyperpolarization-activated current (Ih) blocker ZD 7288 in hippocampal CA1 neurons. *Pflug. Arch.* **435**, 99–106 (1997).
- Maccaferri, G., Mangoni, M., Lazzari, A. & DiFrancesco, D. Properties of the hyperpolarization-activated current in rat hippocampal CA1 pyramidal cells. *J. Neurophysiol.* **69**, 2129–2136 (1993).
- Spruston, N. & Johnston, D. Perforated patch-clamp analysis of the passive membrane properties of three classes of hippocampal neurons. *J. Neurophysiol.* **67**, 508–529 (1992).
- Magee, J. C. Dendritic I_h normalizes temporal summation in hippocampal CA1 neurons. *Nat. Neurosci.* **2**, 508–514 (1999).
- Poolos, N. P., Migliore, M. & Johnston, D. Pharmacological upregulation of h-channels reduces the excitability of pyramidal neuron dendrites. *Nat. Neurosci.* **5**, 767–774 (2002).
- George, M. S., Abbott, L. F. & Siegelbaum, S. A. HCN hyperpolarization-activated cation channels inhibit EPSPs by interactions with M-type K(+) channels. *Nat. Neurosci.* **12**, 577–584 (2009).
- Tsay, D., Dudman, J. T. & Siegelbaum, S. A. HCN1 channels constrain synaptically evoked Ca^{2+} spikes in distal dendrites of CA1 pyramidal neurons. *Neuron* **56**, 1076–1089 (2007).
- Shah, M. M., Anderson, A. E., Leung, V., Lin, X. & Johnston, D. Seizure-induced plasticity of h channels in entorhinal cortical layer III pyramidal neurons. *Neuron* **44**, 495–508 (2004).
- Hardie, J. B. & Pearce, R. A. Active and passive membrane properties and intrinsic kinetics shape synaptic inhibition in hippocampal CA1 pyramidal neurons. *J. Neurosci.* **26**, 8559–8569 (2006).
- Williams, S. R. & Stuart, G. J. Voltage- and site-dependent control of the somatic impact of dendritic IPSPs. *J. Neurosci.* **23**, 7358–7367 (2003).
- Lamsa, K., Heeroma, J. H. & Kullmann, D. M. Hebbian LTP in feed-forward inhibitory interneurons and the temporal fidelity of input discrimination. *Nat. Neurosci.* **8**, 916–924 (2005).

20. Mittmann, W., Koch, U. & Häusser, M. Feed-forward inhibition shapes the spike output of cerebellar Purkinje cells. *J. Physiol.* **563**, 369–378 (2005).
21. Magee, J. C. Dendritic hyperpolarization-activated currents modify the integrative properties of hippocampal CA1 pyramidal neurons. *J. Neurosci.* **18**, 7613–7624 (1998).
22. Williams, S. R. & Stuart, G. J. Site independence of EPSP time course is mediated by dendritic I_h in neocortical pyramidal neurons. *J. Neurophysiol.* **83**, 3177–3182 (2000).
23. Lupica, C. R., Bell, J. A., Hoffman, A. F. & Watson, P. L. Contribution of the hyperpolarization-activated current (I_h) to membrane potential and GABA release in hippocampal interneurons. *J. Neurophysiol.* **86**, 261–268 (2001).
24. Chevaleyre, V. & Castillo, P. E. Assessing the role of I_h channels in synaptic transmission and mossy fiber LTP. *Proc. Natl Acad. Sci. USA* **99**, 9538–9543 (2002).
25. Aponte, Y., Lien, C. C., Reisinger, E. & Jonas, P. Hyperpolarization-activated cation channels in fast-spiking interneurons of rat hippocampus. *J. Physiol.* **574**, 229–243 (2006).
26. Southan, A. P., Morris, N. P., Stephens, G. J. & Robertson, B. Hyperpolarization-activated currents in presynaptic terminals of mouse cerebellar basket cells. *J. Physiol.* **526** (Pt 1), 91–97 (2000).
27. Nolan, M. F. *et al.* A behavioral role for dendritic integration: HCN1 channels constrain spatial memory and plasticity at inputs to distal dendrites of CA1 pyramidal neurons. *Cell* **119**, 719–732 (2004).
28. Nolan, M. F. *et al.* The hyperpolarization-activated HCN1 channel is important for motor learning and neuronal integration by cerebellar Purkinje cells. *Cell* **115**, 551–564 (2003).
29. Pouille, F., Marin-Burgin, A., Adesnik, H., Atallah, B. V. & Scanziani, M. Input normalization by global feedforward inhibition expands cortical dynamic range. *Nat. Neurosci.* **12**, 1577–1585 (2009).
30. Rivera, C. *et al.* The K^+/Cl^- co-transporter KCC2 renders GABA hyperpolarizing during neuronal maturation. *Nature* **397**, 251–255 (1999).
31. Glickfeld, L. L., Roberts, J. D., Somogyi, P. & Scanziani, M. Interneurons hyperpolarize pyramidal cells along their entire somatodendritic axis. *Nat. Neurosci.* **12**, 21–23 (2009).
32. Kaila, K., Voipio, J., Paalasmaa, P., Pasternack, M. & Deisz, R. A. The role of bicarbonate in GABA_A receptor-mediated IPSPs of rat neocortical neurones. *J. Physiol.* **464**, 273–289 (1993).
33. Gullledge, A. T. & Stuart, G. J. Excitatory actions of GABA in the cortex. *Neuron* **37**, 299–309 (2003).
34. Wang, X. J. & Buzsáki, G. Gamma oscillation by synaptic inhibition in a hippocampal interneuronal network model. *J. Neurosci.* **16**, 6402–6413 (1996).
35. Vida, I., Bartos, M. & Jonas, P. Shunting inhibition improves robustness of gamma oscillations in hippocampal interneuron networks by homogenizing firing rates. *Neuron* **49**, 107–117 (2006).
36. Stiefel, K. M., Wespát, V., Gutkin, B., Tegnér, F. & Singer, W. Phase dependent sign changes of GABAergic synaptic input explored in-silico and in-vitro. *J. Comput. Neurosci.* **19**, 71–85 (2005).
37. Bender, R. A. *et al.* Differential and age-dependent expression of hyperpolarization-activated, cyclic nucleotide-gated cation channel isoforms 1–4 suggests evolving roles in the developing rat hippocampus. *Neuroscience* **106**, 689–698 (2001).
38. van Welie, I., van Hooft, J. A. & Wadman, W. J. Homeostatic scaling of neuronal excitability by synaptic modulation of somatic hyperpolarization-activated I_h channels. *Proc. Natl Acad. Sci. USA* **101**, 5123–5128 (2004).
39. Chen, K. *et al.* Persistently modified h-channels after complex febrile seizures convert the seizure-induced enhancement of inhibition to hyperexcitability. *Nat. Med.* **7**, 331–337 (2001).
40. Jung, S. *et al.* Progressive dendritic HCN channelopathy during epileptogenesis in the rat pilocarpine model of epilepsy. *J. Neurosci.* **27**, 13012–13021 (2007).
41. Marcelin, B. *et al.* h channel-dependent deficit of theta oscillation resonance and phase shift in temporal lobe epilepsy. *Neurobiol. Dis.* **33**, 436–447 (2009).
42. Schuchmann, S. *et al.* Experimental febrile seizures are precipitated by a hyperthermia-induced respiratory alkalosis. *Nat. Med.* **12**, 817–823 (2006).
43. Kyrozis, A. & Reichling, D. B. Perforated-patch recording with gramicidin avoids artifactual changes in intracellular chloride concentration. *J. Neurosci. Methods* **57**, 27–35 (1995).
44. Hines, M. L. & Carnevale, N. T. The NEURON simulation environment. *Neural Comput.* **9**, 1179–1209 (1997).
45. Zheng, K., Scimemi, A. & Rusakov, D. M. Receptor actions of synaptically released glutamate: the role of transporters on the scale of nanometers to microns. *Biophys. J.* **95**, 4584–4596 (2008).

Acknowledgments

This work was supported by the Medical Research Council, Epilepsy Research UK and the European Research Council. We are grateful to D. Rusakov, R. Surges and other members of the laboratory for comments and suggestions. We thank M. Shah for kindly providing us with the HCN1 knockout mice and critical reading of the manuscript. We thank K. Zheng for providing the multimode cluster for computations.

Author contributions

I.P. and A.S. designed and performed experiments, analysed data and wrote the paper; L.S. performed modelling; D.M.K. and M.C.W. designed experiments, directed the project and wrote the paper.

Additional information

Supplementary Information accompanies this paper at <http://www.nature.com/naturecommunications>

Competing financial interests: The authors declare no competing financial interests.

Reprints and permission information is available online at <http://npg.nature.com/reprintsandpermissions/>

How to cite this article: Pavlov, I. *et al.* I_h -mediated depolarization enhances the temporal precision of neuronal integration. *Nat. Commun.* **2**:199 doi: 10.1038/ncomms1202 (2011).

License: This work is licensed under a Creative Commons Attribution-NonCommercial-Share Alike 3.0 Unported License. To view a copy of this license, visit <http://creativecommons.org/licenses/by-nc-sa/3.0/>